

# Experimental and numerical analysis of solar still using Pyrex glass quantum dot in tropical climate

Pranav Kumar Singh<sup>1</sup> | Pushendra Kumar Singh Rathore<sup>1,2</sup>  | Shailendra Kumar Shukla<sup>1</sup>

<sup>1</sup>Center for Energy and Resources Development, Department of mechanical Engineering, Indian Institute of Technology (BHU), Varanasi, India

<sup>2</sup>Centre for Advanced Studies, Dr. A.P.J. Abdul Kalam Technical University, Lucknow, India

## Correspondence

Shailendra Kumar Shukla, Center for Energy and Resources Development, Department of mechanical Engineering, Indian Institute of Technology (BHU), Varanasi 221005, India.  
Email: skshukla.mec@itbhu.ac.in

## Summary

This study investigates the effect of using quantum dots (QDs) on the performance of solar still in the tropical climate of India. This article presents a new way to use QDs, which on absorbing solar energy increases water evaporation rate. Pyrex glass powder QDs are used in the solar still due to its high absorptivity value. An experimental setup of solar still with QD and without QD was developed, and a comparative analysis was conducted under the real outdoor environment in a tropical climate. The experimental results were also validated through mathematical modeling. The experiment was carried out by mixing Pyrex glass powder QDs with black paint and was coated on the basin and sidewalls of the solar still. Experiments were conducted for a depth of 0.02 m for solar still with QDs and without QDs. The results revealed that for 0.02 m of water depth and 1 m<sup>2</sup> of basin area, the percentage increase in distillate output using Pyrex glass powder QDs is 29.36% experimentally and 29.94% theoretically. Furthermore, the net percentage increase in solar still efficiency by using Pyrex glass QDs is 74.74% experimentally and 61.03% theoretically. The study analyzed that all the experimental results are in good agreement with the theoretical analysis. The addition of Pyrex glass powder QDs and black paint mixture in the basin of solar still caused significant enhancement in the distillate output and solar still efficiency.

## KEYWORDS

distillate output, evaporation, quantum dot, solar still

## 1 | INTRODUCTION

Due to the population explosion in the 21st century, the whole world is facing the problem of water scarcity. Water is abundant in nature, but drinkable water is approximately 2% of total water present on Earth. It is one of the most important contentions among regions, states, and communities. So, the evaluation on the proper use and conservation of water has now become important for sustainable development. The availability of fresh

water varies from location to location on earth. According to the world water development report, there are more than 2.2 billion people who do not have the accessibility of safe drinking water.<sup>1</sup> A study revealed that almost 4 billion people live under water crisis at least 1 month of the year.<sup>2</sup> To mitigate these challenges in a sustainable and cleaner way, the United Nations set “clean water and sanitation” as their one of the important goals.

On Earth's surface, oceans are the largest water bodies. However, seawater is saline and is not fit for drinking. The

seawater has the highest amount of total dissolved solids (TDS), which is in the range of 35 000 to 45 000 ppm, while for land water, the TDS is up to 10 000 ppm. The TDS in water for drinking purpose should not exceed more than 500 ppm (ppm).<sup>3-5</sup> The excess amount of TDS along with impurities in the drinking water causes health problems like stomach problems, bad taste, etc. The distillation process is used for the cleaning and purification of saline water, which have total dissolved solids TDS upto 500 ppm or less. Seawater desalination is the most widely used technology for water purification,<sup>6-8</sup> but it is very costly process and not affordable by everyone. Generally, the technologies that are used for waste water treatment are thermal evaporation, ion water exchange, and osmosis.<sup>9,10</sup> However, these technologies are also expensive and have complex configuration and covers large area for their operation and management. Wastewater treatment technology to remove pollutants like metal ion, detergents, and organic contaminants is also not cost-effective.<sup>11,12</sup> One of the sustainable technologies that have gained much hype in recent years is solar-enabled purification, called solar distillation.<sup>13,14</sup> Solar distillation is one of the techniques which use solar thermal energy to distillate the water with the help of a component known as solar still. Since, solar radiation for thermal applications is available in abundant quantity throughout the year in tropical countries like India, and because of various merits associated with solar energy, it can be easily and effectively used for solar distillation.<sup>15</sup> However, the low productivity of solar still limits its applicability for distillation. Many studies have been carried out to evaluate and enhance the productivity of solar still.

A study shows experiment with transparent side walls and honeycomb structure in the basin on single slope solar still (SSSS) so that there is an increase in evaporation rate, which increases yield up to 2.61 L/m<sup>2</sup>day.<sup>16</sup> A study shows an experiment with a baffled absorber plate that was put in the basin of solar still; the productivity is 20% higher than conventional still.<sup>17</sup> A different study investigated the impact of using side mirrors and sun tracking in active and passive modes. In passive mode, the maximum fresh water with only sun tracking was 1.90 L compared to conventional passive solar still, which has productivity of 1.53 L. The maximum quantity of freshwater with sun tracking and mirror was found to be 2.19 L.<sup>18</sup> One study conducted the experiment with inclined solar still with wick material on different absorber configurations (stepped wire mesh plate, stepped plate, and flat plate). The maximum yield obtained is upto 4.28 L/day. The main drawback with wick type solar still is that it does not work at night.<sup>19</sup> An experiment was performed by taking corrugated sheets (CSs) as absorber material and granite gravel as a sensible heat storage material (SHSM) on conventional solar still with triple basin, which has

evacuated heat pipes. The productivity of solar still is around 19 L/m<sup>2</sup>/day.<sup>20</sup> A comparative analysis between conventional solar still, conventional pyramidal solar still, and modified pyramidal solar still (using CuO and carbon black nanofluids and evacuated tube) was conducted. This study found that the improvement in distillate output increased by 27.75% when CuO nanofluid is used while there is 33.59% increase in output by using carbon black nanofluid. The maximum solar still efficiency is 64.5 for modified pyramidal solar still with carbon black nanoparticles.<sup>21</sup> An experiment was performed by using phase change material along with solar concentrating unit under desert condition. The concentrator unit is used to heat the brackish water, which then goes to conical distiller where they have used paraffin wax as a PCM to absorb heat from brackish water. They found that with the addition of PCM, the increase in system productivity, system efficiency, and concentrating efficiency was 783%, 157.8%, and 157.8%, respectively, and also increase in working hour of distillation system.<sup>22</sup>

Researchers have used different types of materials to enhance the distillate output of still. A study used nanofluid in the basin. The distilled output is 5.25 L, while by using nanofluid in the basin and nano paint on the glass, the yield is 5.56 L.<sup>23</sup> Another experiment used Al<sub>2</sub>O<sub>3</sub> nanoparticle of varying concentration in the basin of solar still. They observed that by using nanoparticle, the distilled output is increased by 2.6%, 7.2%, 12.3%, and 17.6% for weight concentrations of 0.2%, 0.10%, 0.05%, and 0.01%, respectively, in comparison with solar still without nanoparticles.<sup>24</sup> Single-basin dual-slope solar still along with Al<sub>2</sub>O<sub>3</sub> with varying depth of 0.010, 0.020, and 0.030 m was used for experiment. Enhanced productivity of 1.252, 1.220, and 1.120 L was observed in comparison to conventional solar still, which has distillate output 0.989, 0.950, and 0.938 L with a depth of 0.010, 0.020, and 0.030 m, respectively.<sup>25</sup> An investigation on SSSS by adding nanofluid of Al<sub>2</sub>O<sub>3</sub>/water with varying concentrations (0.05% and 0.1% volume fraction) and integrated with parabolic trough collector was conducted. The study reveals that the maximum yield is 1.741 L with 0.1% volume fraction of Al<sub>2</sub>O<sub>3</sub>/water nanofluid with a basin area of 1 m<sup>2</sup> and water depth of 0.025 m. There is 66% increase in distillate output and solar still efficiency is increased by 70% with this modification.<sup>26</sup> TiO<sub>2</sub> nanoparticles mixed with Cr<sub>2</sub>O<sub>3</sub> along with different combinations of hybrid bond absorption were used to enhance the performance of solar still. The average daily distillate output of still is 7.89 and 5.39 L/m<sup>2</sup> during summer and winter, respectively.<sup>27</sup> An experiment was conducted on solar still in which CuO nanoparticle was implanted with paraffin on V-corrugated plate and the distillate output of different nanoparticles of 0.3%, 0.2%,

and 0.1% by weight was 0.510, 0.455, and 0.440 L/0.25 m<sup>2</sup>/day, respectively.<sup>28</sup> A study has performed with weir-type solar still in which PCM material is used. They used paraffin as PCM material due to which 4.35% of increment in annual productivity compared to conventional solar still was achieved.<sup>29</sup> A study did the experiment to analyze the performance of solar still using Kanchey marble, which acts as a sensible storage material in the solar still. They found out that the yield with Kanchey material was 4.094 L/m<sup>2</sup>/day, which is 16.32% more than conventional solar still.<sup>30</sup> A study did the experiment on pyramidal solar still by using TiO<sub>2</sub> nano black paint on the absorber plate, the yield is 6.6 kg/m<sup>2</sup>.<sup>31</sup> The author has performed the experiment with SSSS by perturbation of water surface. Perturbation is achieved by injecting air bubbles in the water basin, which produces surface ripple, which enhances evaporative surface area and also helps to increase mass transfer coefficient. The total distillate yield was 6.137 L/m<sup>2</sup>.<sup>32</sup> A study investigates the performance of solar still with different heat storage material in upper basin of double slope solar still with vacuum tubes. The productivity with pebbles was 9.34 kg, with granite gravel the productivity was 9.86 kg, and with calcium stones, it was 10.42 kg in summer days.<sup>33</sup> A study presents several experiments using different material to enhance the performance of solar still. One experiment used black dye in which the distillate output was 3.7 L/m<sup>2</sup>/day. In another experiment, black rubber mat was used where the distillate output was 3.3 L/m<sup>2</sup>/day. Black ink was also used in which the distilled output was 3 L/m<sup>2</sup>day.<sup>34</sup> Similar experiment was performed by using black dye in conventional solar still (CSS); the productivity was 3.4 L/m<sup>2</sup>/day, and in other experiment, he used black dye with regenerative solar still, the yields was 4.2 L/m<sup>2</sup>day.<sup>35</sup> A study presents the analysis by using Paraffin wax as a phase change material in the concentrating solar heater. They have performed following experiments: (a) Using water as an absorber material and without solar tracker, (b) using water as an absorber material and with solar tracking, (c) using PCM as a thermal storage material without solar tracker, and (d) using PCM as thermal storage material and with solar tracker. They found that the system working time is increased by 3 hours by adding PCM without solar tracker, and the system productivity is enhanced by 180% while when they used both PCM and solar tracker then the system working time is enhanced by 3 hours, and the system productivity is enhanced by 307.54%.<sup>36</sup> A study shows comparative analysis of SSSS in three different ways that is, (i) simple solar still with thermoelectric heating (TEH) in basin, (ii) simple solar still with TEH and silver nanofluid with 0.03% by weight in the basin, (iii) simple solar still with TEH, silver nanofluid, and

double slope symmetrical external condenser. They found that the maximum yield of 7.760 L/m<sup>2</sup>/day when TEH, silver nanofluid, and double slope symmetrical external condenser is incorporated simultaneously.<sup>37</sup> An experiment was performed on single slope solar distiller. They have analyzed (a) conventional solar still without any modification, (b) using paraffin as a PCM in the solar still, and (c) using combination of paraffin wax with nano-Al<sub>2</sub>O<sub>3</sub>. They found that by adding Paraffin wax the productivity is increased up to 10.38% while when the combination of paraffin wax with nano-Al<sub>2</sub>O<sub>3</sub> is used then the productivity of the system is increased by 60.53% in comparison to conventional solar still.<sup>38</sup>

It has been found that various studies have analyzed the effect on distillate output and efficiency of solar still by using nano-particles and heat storage techniques. Currently, nano-technology is emerging as a new field, and researchers are trying to use nano-material for enhancing the performance of solar still. QDs is also part of nano-material. QDs are semiconductor crystals with a diameter of 1 to 10 nm. The most important characteristics of QDs polymer and composites are their size, photo bleaching stability, luminance, bio compatibility, low toxicity, and optical property. Due to its various properties, researchers are trying to use it for various applications like in biomedical, light emitting diodes, photovoltaic, catalysis, photo-detector, and photoconductor.<sup>39</sup> However, a limited amount of work has been reported by using QD for solar thermal applications. Most work on the use of quantum dots for harnessing solar energy is carried out by PV cells for conversion of solar energy into electrical energy. Furthermore, no study was carried out on evaluating the effect of QD on the performance of solar still. In this study, a novel approach of enhancing the performance of solar still in the tropical environment is presented. Two solar still was developed to conduct this study. The basin of one solar still was coated with Pyrex glass QD, while the basin of another solar still is without QDs. A comparative investigation of both the solar still in terms of distillate output, temperature of glass, and efficiency of solar still was conducted in real outdoor tropical climate of India. Additionally, a mathematical model was also developed to validate the experimental findings. The research work on the solar still with QDs provides a new way to enhance the performance of passive type solar still.

## 2 | METHODOLOGY

This study consists of experimental work and mathematical modeling to evaluate the effect of QDs on the performance of solar still. Two similar solar still, one with QDs and the other without QDs, was fabricated at the roof of

the CERD (Centre for energy and resource development) lab of Mechanical engineering Department, IIT (BHU), Varanasi (25.3176°N, 82.9739°E). The location has typical tropical-type environment having plenty of solar radiation throughout the year. The experiment was conducted, and data were collected for 28 Oct, 2020, from 9:30 AM to 5:30 PM and. For the calculation purpose 1-day data are easier to analyze and validate with experimental results. The solar still was tilted at around 25° to collect maximum solar radiation, and the depth of water was taken as 0.02 m. Since we are analyzing and comparing the distillate output, we can take any value for depth of water as per suitability of given set-up. So, we have taken the same depth of water for both the setups.

As shown in Figure 1, when the solar radiation incident on the basin water, the evaporation of water takes place. The evaporated vapor from the basin is condensed to liquid. The condensation of liquid water takes place on the surface of the glass cover, which was exposed toward the side of basin water. Because of the slope of the glass cover, the condensed water moves to the channel and a passage having diameter of 0.01 m was drilled in the middle of the channel in the front of the basin through which fresh water is collected in the flask. We have coated Pyrex glass QDs in the basin, which results in an increase of the absorptivity of the basin due to which there is increase in the water temperature in the basin. Increase in water temperature results in the increase of the evaporation rate. Because of the increase in evaporation rate, the distillate output also increases. Pyrex glass QDs has the ability to absorb heat and we are taking advantage of this absorption property. In present work, QD paint has been prepared by mixing Pyrex glass QDs and black paint. This mixture was then coated onto the surface of the basin, which improves the energy absorbing capacity of solar still. During the experiment, various parameters like temperature of basin water, temperature of glass cover, and output of solar still are measured and recorded for every 1 hour from 9:30 AM to 5:30 PM. The

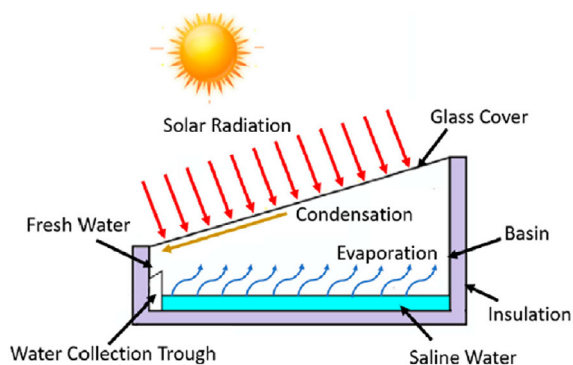


FIGURE 1 Schematic diagram of solar still<sup>40</sup>

recorded data of both the solar still were analyzed, and a comparative performance evaluation was presented.

### 3 | MATHEMATICAL MODELING

The assumptions for mathematical analysis of solar still are following:

1. The specific heat capacity of plain glass cover is very small, so we can neglect its effect for our calculation.
2. Whole set-up is leakage proof.
3. The heat transfer through side wall and back wall is assumed to be negligible, so only one directional heat transfer takes place which is from cover to basin
4. There is no heat loss through side walls
5. The intensity is taken as the average intensity value for 1 step hour.

Applying energy balance on glass surface, we get

$$h_{gw} (T_w - T_g) = h_{ga} (T_g - T_a) \quad (1)$$

Applying energy balance on water, we get

$$\alpha_w I(t) + h_{bw} (T_b - T_w) = (MC)_w d/dt(T_w) + h_{gw} (T_w - T_g) \quad (2)$$

Applying energy balance on basin, we get

$$\alpha_b I(t) = h_{bw} (T_b - T_w) + h_{ba} (T_b - T_a) \quad (3)$$

By rearranging Equation (1), we get

$$T_g = [h_{gw}^* T_w + h_{ga}^* T_a] / (h_{gw} + h_{ga}) \quad (4)$$

By rearranging Equation (3), we get

$$T_b = \alpha_b I(t) + h_{bw}^* T_w + [h_{ba}^* T_a / (h_{bw} + h_{ba})] \quad (5)$$

By rearranging Equation (2) and putting value of  $T_g$  and  $T_b$  in terms of  $T_w$  and  $T_a$ , we get

$$\begin{aligned} & (MC)_w d/dt(T_w) \\ & + (h_{bw}^* h_{ba} / h_{bw} + h_{ba} + h_{gw}^* h_{ga} / h_{gw} + h_{ga})^* T_w \\ & = \alpha_w I(t) + h_{bw} / h_{bw} + h_{ba} (\alpha_b I(t) + h_{ba} T_a) \\ & + (h_{gw} h_{ga} / h_{gw} + h_{ga})^* T_a \end{aligned} \quad (6)$$

Calculation of  $h_{gw}$  between glass and water,

$$h_{gw} = h_{\text{radiation,g-w}} + h_{\text{convection,g-w}} + h_{\text{evaporation,w-g}}$$

The co-efficient of radiative heat transfer ( $h_{\text{radiation,g-w}}$ ) is given by Duffie and Beckman.<sup>41</sup>

$$h_{\text{radiation,g-w}} = \epsilon_{\text{effective}} \sigma (T_w^2 + T_g^2) (T_w + T_g) \quad (7)$$

where,  $\epsilon_{\text{effective}}$  is the emmissivity computed as follows

$$\epsilon_{\text{effective}} = 1/\epsilon_w + 1/\epsilon_g - 1 \quad (8)$$

As the process of evaporation–condensation is taking place simultaneously, Dunkle's equation is used<sup>42</sup>:

$$h_{\text{convection,w-g}} = 0.884 [T_w - T_g + (P_w - P_g) * T_w / (268.9 * 10^3 - P_w)]^{1/3} \quad (9)$$

$$h_{\text{evaporation,w-g}} = 16.276 * 10^{-3} * h_{\text{convection,w-g}} * P_w - P_g / T_w - T_g \quad (10)$$

$P_w$  denotes the value of vapor pressure corresponding to basin water temperature, and  $P_g$  denotes the value of vapor pressure corresponding to the glass temperature, and we can find out their value by using following relation:

$$\text{where, } P_w \text{ (water vapor pressure corresponding to } T_w) = e^{(25.317 - 5144/T_w)} \quad (11)$$

$$P_g \text{ (water vapor pressure corresponding to } T_g) = e^{(25.317 - 5144/T_g)} \quad (12)$$

$$h_{ga} = h_{\text{radiation,g-sky}} + h_{\text{convection,g-air}}$$

By using Duffie–Beckman relation which gives the co-efficient of radiative heat transfer  $h_{\text{radiative,g-sky}}$ , between the sky and the cover.<sup>41</sup>

$$h_{\text{radiation,g-sky}} = \epsilon_g * \sigma * (T_g^2 + T_{\text{sky}}^2) (T_g + T_{\text{sky}}) \quad (13)$$

where the temperature of sky ( $T_{\text{sky}}$ ) is given by following.<sup>43</sup>

$$T_{\text{sky}} = 0.0552 T_a^{1.5} \quad (14)$$

The co-efficient of the convective heat transfer  $h_{\text{convection,g-air}}$  is a function of wind velocity and is obtained by following relation:

$$h_{\text{convection,g-air}} = 2.8 + 3V, \text{ where } V \text{ is average velocity of wind which is in m/s} \quad (15)$$

$$h_{bw} = C * k * [Gr * Pr]^{1/n} \quad (16)$$

For free convection the heat transfer correlation is given by.<sup>44</sup>

$$C = 0.54, n = 1/4, \text{ for } 10^4 < Ra_L < 10^7; \quad (17)$$

$$C = 0.15, n = 1/3, \text{ for } 10^7 < Ra_L < 10^{10}; \quad (18)$$

$L$  = area/perimeter;

The Grashof number is given by.<sup>45</sup>

$$Gr = g * \beta_w * \Delta T * L_c^3 / \nu_w^2 \quad (19)$$

$$Pr = c_{pw} * \mu_w / k_w \quad (20)$$

where,  $\Delta T = T_w - T_b$ ;  $L_c$  = area/perimeter.

The heat transfer coefficient between basin and air is computed as Fourier equation of conduction:

$$h_{ba} = k_b / L_b + [L_{in} / k_{in} + 1 / h_{air}]^{-1} \quad (21)$$

For our case, we have taken,

$$\epsilon_w \text{ (Emissivity of water)} = 0.9,^{46}$$

$$\epsilon_g \text{ (Emissivity of window glass)} = 0.9,^{47}$$

$M_w$  (mass of water) = 20 kg (we maintain the same level of water in the basin),

$$C_w = 4.18 * 10^3 \text{ J/kg K},^{48}$$

$$\sigma = 5.67 * 10^8 \text{ W/m}^2 \text{ T}^4, g = 10 \text{ m/s}^2, L = L_c = A_s / P_s = 0.25 \text{ m}, V \text{ (average velocity of wind)} = 7.6 \text{ m/s},$$

$$A_s \text{ (area of basin)} = 1 \text{ m}^2 \text{ (1m length and 1 m breadth)}$$

$\beta_w = 385 * 10^{-6} \text{ 1/K}$ ,<sup>49</sup> it depends on temperature but variation is not much for a range of temperature, so we can assume it as constant for our analysis.

$\nu_w = 0.615 * 10^{-6} \text{ m}^2/\text{s}$ ,<sup>50</sup> as kinematic viscosity depends on temperature, but it does not vary much, so we can assume it as constant for our analysis.

$k_w = 0.62$ <sup>51</sup> Thermal conductivity of water depends on temperature, but we can assume it constant for our analysis.

$$\Delta T > 0,$$

$k_b$  (Thermal conductivity of basin) = 0.8 (FRP without quantum dot).

$k_b$  (Thermal conductivity of basin) = 0.82 (FRP with quantum dot coating).

$k_{in}$  (thermal conductivity of wool) = 0.03 w/m K,<sup>52</sup>

$L_{in} = 0.07$  m,  $\alpha_w = 0.85$ ,

$\alpha_b$  (Absorptivity of basin or fraction of solar energy absorbed by basin) = 0.68 (FRP without QD).

$\alpha_b$  (Absorptivity of basin or fraction of solar energy absorbed by basin) = 0.98 (FRP with QD).

$h_{air} = 13.75$  W/m<sup>2</sup> K. These data are shown in Table 1.

**TABLE 1** Different data that are used for mathematical modeling of solar still

$A_s$ = area of basin (in m <sup>2</sup> )	1
$P_s$ = perimeter of basin (in m)	4
$L_c$ = Characteristic length of basin (in m)	0.25
$L_b$ = Thickness of basin (in m)	0.01
$L_{in}$ = Thickness of insulation material (in m)	0.07
$M_w$ = Mass of water (in kg)	20
$C_w$ = Specific heat capacity of water (in J/kg-K)	4.18*10 <sup>3</sup>
$h_{air}$ = Average heat transfer co-efficient of air (free convection in W/m <sup>2</sup> K)	13.75
(MC) <sub>w</sub> = Product of mass of water and specific heat of water (J/K)	83.6*10 <sup>3</sup>
$V$ = Average velocity of air used for calculation (m/s)	7.6
$k_b$ = Thermal conductivity of basin (W/m K)[for FRP in SS]	0.8
$k_b$ = Thermal conductivity of basin (W/m K)[for QD]	0.82
$k_w$ = Thermal conductivity of water (W/m K)	0.62
$k_{in}$ = Thermal conductivity of wool (W/m K)	0.03
$\nu_w$ = Kinematic viscosity of water	0.615*10 <sup>-6</sup>
$\alpha_w$ = Absorptivity value of water or fraction of solar energy absorbed by water (dimensionless)	0.85
$\epsilon_w$ = Emissivity value of water (dimensionless)	0.9
$\epsilon_g$ = Emissivity value of glass (dimensionless)	0.9
$\alpha_b$ = Absorptivity of basin or fraction of solar energy absorbed by basin (dimensionless) [for FRP]	0.68
$\alpha_b$ = Absorptivity value of basin or fraction of solar energy absorbed by basin (dimensionless) [for QD]	0.99
$\beta_w$ = Coefficient of volumetric thermal expansion (K <sup>-1</sup> )	385*10 <sup>-6</sup>
$\sigma$ = Stefan-Boltzman constant (W/m <sup>2</sup> K <sup>4</sup> )	5.67*10 <sup>8</sup>

FRP, fiber-reinforced plastics; QD, quantum dots.

So by calculation,  $Ra_L$  is in range of (10<sup>7</sup>-10<sup>10</sup>), so we use Equation (18) for our analysis of heat transfer coefficient between basin and water.

We can take an average value of intensity in 1 step hour period for our analysis.

Since  $h_{b-w}$  is not changing much so we can assume it to be constant for our whole analysis.

So our Equation (6) will look like,

$$d/dt(T_w) + a T_w = c \quad (22)$$

where  $a = 1/(MC)_w[h_{bw}*h_{ba}/h_{bw} + h_{ba} + h_{gw}*h_{ga}/h_{gw} + h_{ga}]$ ;

$$c = 1/(MC)_w[[\alpha_w + (h_{bw}* \alpha_b/h_{bw} + h_{ba})]I(t) + [h_{bw}*h_{ba}/h_{bw} + h_{ba} + h_{gw}*h_{ga}/h_{gw} + h_{ga}]T_a]$$

so  $a$  and  $c$  are constant value for 1step hour and the solution of the Equation (22) is

$$T_w^{i+1} = T_w^i e^{-3600a} + c*[1 - e^{-3600a}]/a \quad (23)$$

$$T_g^{i+1} = h_{gw}*T_w^{i+1} + h_{ga}*T_a^{i+1}/(h_{gw} + h_{ga}) \quad (24)$$

$$T_b^{i+1} = \alpha_b I(t)_{average}^i + h_{bw} T_w + h_{ba} T_a / (h_{bw} + h_{ba}) \quad (25)$$

$I(t)_{average}^i$  = average intensity for  $i$ th period.

The evaporative heat transfer rate and distillate output (hourly basis) are given by Equations (26) and (27) respectively:

$$Q_{evaporative} = h_{evaporation,g-w}*(T_w - T_g) A_s \quad (26)$$

$$m_{evaporation} \text{ (theoretical output of water in ml)} \\ = [h_{evaporation,g-w}*(T_w - T_g)*A_s*3600/\text{Latent Heat}]*10^3 \quad (27)$$

The Solar still efficiency can be determined by:

$$\eta_i = h_{evaporation,g-w} (T_w - T_g) / I(t) \quad (28)$$

## 4 | SOLUTION TO MATHEMATICAL MODEL

As we have observed that  $T_w$ ,  $T_g$ ,  $T_a$ ,  $N_i$  value changes with time. In the above calculation, a numerical method has been used. For our numerical analysis, we have used the time interval  $\Delta t$  as 1 hour. The following steps have followed for numerical analysis:

1. First, we initialize the value of  $T_w$ ,  $T_g$ , and  $T_a$  solar still specifications and other climatic parameters, and then we calculate various heat transfer coefficients value.
2. After calculating various heat transfer coefficient values, we predict the next value of  $T_w$  and  $T_g$  using previous heat transfer coefficients by using Equations (23) and (24) and distillate output is calculated using Equations (26) and (27).
3. When we get new values of  $T_w$  and  $T_g$ , the new value of heat transfer coefficients is calculated, and step 2 is repeated for next time interval.
4. For a given time interval  $\Delta t$ , the value of  $T_g$ ,  $T_w$ , and  $T_a$  and heat transfer coefficient values are assumed to be constant for each interval of time, and as a result, the total distillate output is calculated.
5. For a given time interval  $\Delta t$ , the solar still efficiency for  $i$ th period ( $\eta_i$ ) is obtained by using Equation (28).

## 5 | EXPERIMENTAL SET-UP

The solar still with a basin, which is of square shape with an area of  $1\text{ m}^2$  ( $1\text{ m} \times 1\text{ m}$ ) and thickness of  $0.01\text{ m}$  is used. Side walls which are of triangular shape having base, height, and thickness of  $1$ ,  $0.45$ , and  $0.01\text{ mm}$ , respectively, and back wall, which is of rectangular shape having length, height, and thickness of  $1$ ,  $0.45$ , and  $0.01\text{ m}$ , respectively. The basin side wall and back wall are made up of fiber-reinforced plastics (FRP), which has thermal conductivity value of  $0.8\text{ W/m}\cdot\text{K}$  and absorptivity value in the range of  $0.6$  to  $0.7$ . In one setup, only FRP is used as basin material, and in the second setup, black paint with glass powder quantum dot, as shown in Figure 2, was coated on FRP. The detailed dimensional view of the solar still developed to conduct the experiment is shown in Figure 3.

Glass powder QDs were procured from Center for Material for Electronics Technology (C-MET), Pune, Ministry of Electronics and Information Technology, India, as shown in Figure 4. The value of its thermal

conductivity is around  $0.82\text{ W/m}\cdot\text{K}$ , and absorptivity value is in the range of  $0.95$  to  $0.99$ , respectively. Plain window glass is used as a glass cover, which has transmissivity of  $0.9$  and length, breadth, and thickness of  $1.10$ ,  $1$ , and  $0.005\text{ m}$ , respectively. Insulation, by using glass wool, was done around the side wall, back wall, and bottom of basin to minimize the heat loss to the surrounding. Glass wool has thermal conductivity of  $0.03\text{ W/m}\cdot\text{K}$ , and thickness of  $0.07\text{ m}$  is used as insulating material.

The four iron rods each of height  $0.15\text{ m}$ , which were welded below the basin of solar still, act as support for still. The whole set-up was put on a cement foundation with some part of the iron stand in the cement. The length, breadth, and height of cement foundation are  $1.30$ ,  $0.22$ , and  $0.30\text{ m}$  respectively. The productivity of solar still is a function of the temperatures of basin water and the inner glass temperature. So, thermocouple is fixed on cover glass and on glass basin to record the value of temperature. The glass cover temperature, basin temperature, water temperature, and surrounding temperature were measured by K-type thermocouple. Pyranometer was used to measure the solar intensity, which was coming from the sun. Pyranometer has accuracy of  $\pm 25\text{ W/m}^2$ , and its working range is between  $0$  and  $1750\text{ W/m}^2$ . The comparative analysis of productivity and efficiency of simple solar still and solar still with quantum dot has been analyzed at the water depth of  $0.02\text{ m}$ . Wind velocity is measured by an instrument named anemometer. The intensity and wind velocity data with time on Oct 28, 2020, are shown in Figure 5. We can also say from Figure 3 that the variation of intensity and wind velocity depends on the external environment. Wind velocity is more uniform than intensity on Oct 28, 2020. There is a sudden drop in intensity from  $856$  to  $300\text{ W/m}^2$  at  $13:30$  hours due to sudden clouds formation in the sky. However, soon clouds disappear, and solar intensity increases from  $300$  to  $499\text{ W/m}^2$ . The specifications of measuring instrument are shown in Table 2.



**FIGURE 2** Experimental set up of solar still A, without Quantum Dot B, with glass powder Quantum dot

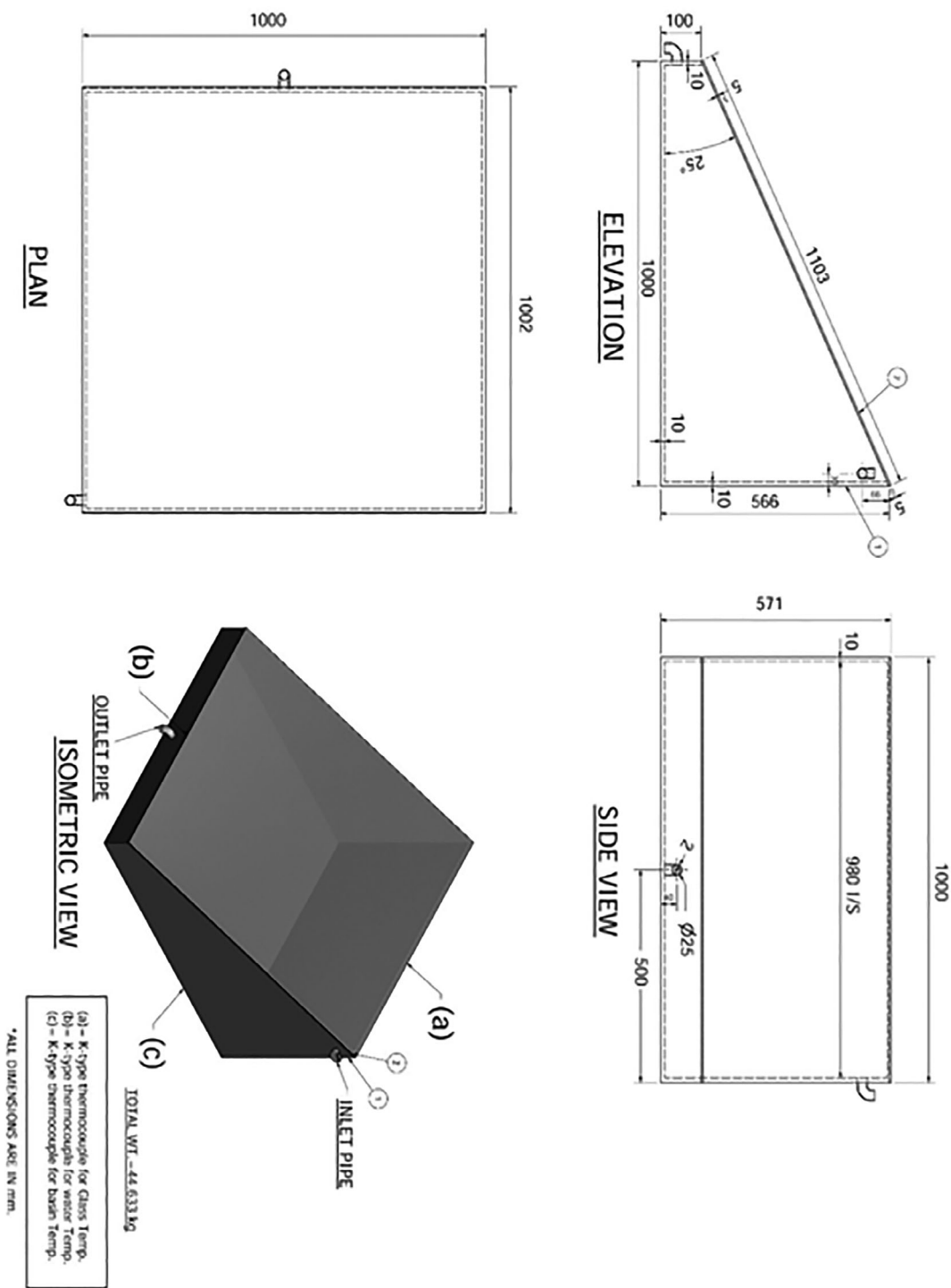


FIGURE 3 Dimensional view and isometric view of the solar still

## 6 | RESULT AND DISCUSSION

The temperature distribution of water, which is measured by thermocouple and also theoretical temperature prediction in SSSS and SSSS with QD, is shown in Figure 6. From the graph, we can say that for a depth of 0.02 m when simple solar still is used, the absorber plate

has reached the highest temperature around 51°C at 13:30 hours and theoretically highest around 50°C at 12:30 hours. When Pyrex glass QD with black paint is used in the basin of solar still for depth of 0.02 m, then the highest temperature experimentally was around 54°C at 12:30 hours, and theoretically the highest temperature was around 52°C. The temperature of water recorded in

**FIGURE 4** A, Pyrex glass powder quantum dots (QD) and B, black paint with Pyrex glass powder QD

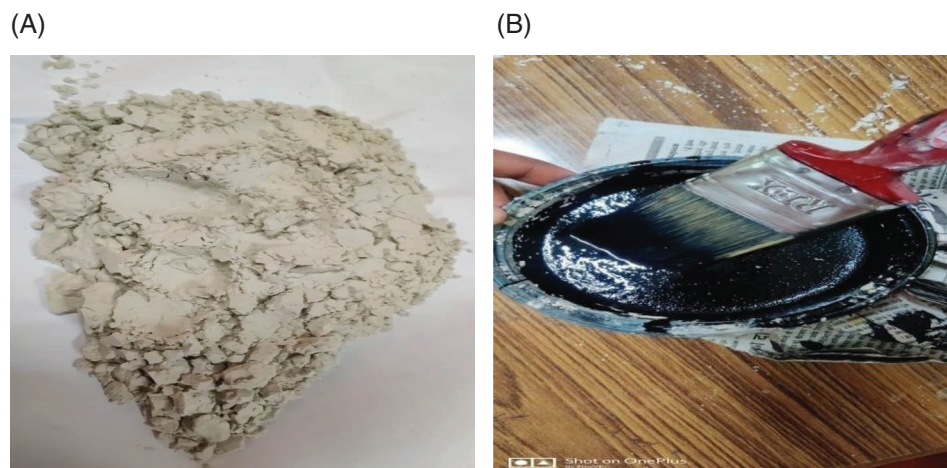


**FIGURE 5** Solar radiation intensity and wind velocity with time

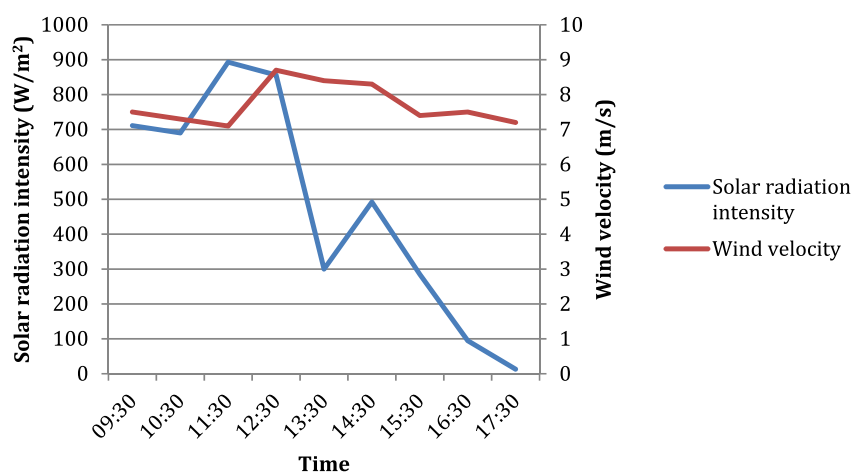


**TABLE 2** Name and Specification of Measuring Instruments

Device	Range	Standard uncertainty
K-class thermocouple	-100°C to 1300°C	0.06°C
Pyranometer	0–1750 W/m <sup>2</sup>	+25 W/m <sup>2</sup> to –25 W/m <sup>2</sup>
Anemometer	0.3–30 m/s	+5% to –5%

solar still with Pyrex glass QD is higher in comparison to temperature of water recorded in SSSS. This has happened because Pyrex glass QD has increased the absorption of solar energy in the basin which increases the water temperature higher than SSSS.

Figure 7 shows the temperature distribution of inner side of the glass and theoretical temperature prediction in SSSS and SSSS with QD. From the graph, it has been observed that for the depth of 0.02 m, for simple solar

still, the glass has the highest temperature of 46°C at 13:00 hours, and theoretically the highest temperature was around 43.14°C at 12:30 hours. When Pyrex glass quantum dot with black paint is used in a basin of solar still for depth of 0.02 m, then the highest temperature of glass achieved was around 44°C at 12:30 hours, and theoretically highest temperature was around 45°C at 13:30 hours.

Figure 8 shows the distillate output (in ml) on hourly basis of SSSS and SSSS with QD experimentally and theoretically. The maximum distillate output experimentally in simple solar still was 0.260 L at 13:30 hours at an average intensity of 578 W/m<sup>2</sup>, and theoretical maximum output in solar still (SS) was 0.1809 L at 12:30 PM at an average intensity of 874.5 W/m<sup>2</sup>. When SS with QD is used, then the maximum distillate output (in mL) obtained experimentally is 0.310 L at 13:30 hours and theoretical maximum output with QD (in mL) was 0.28645 mL at 13:30 hours at an average intensity of 578 W/m<sup>2</sup>. This was happened because when Pyrex glass QD was used, it increases the absorption coefficient of

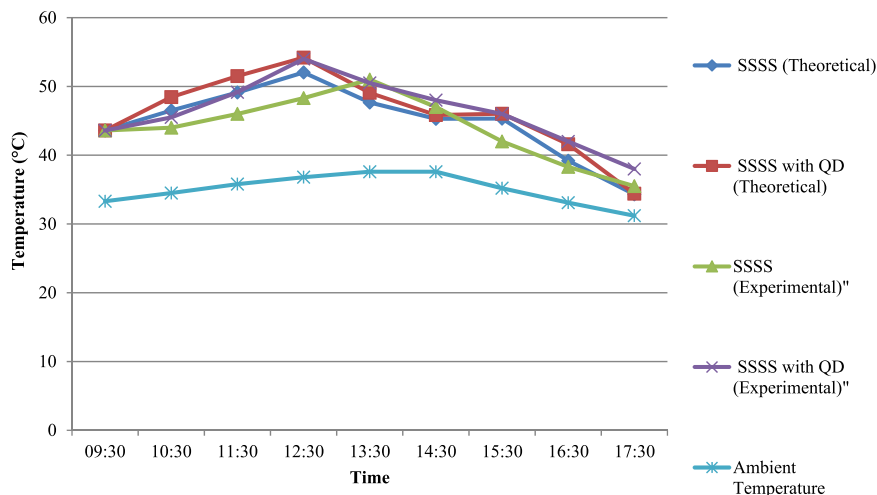


FIGURE 6 Maximum temperature of water (in °C) in single slope solar still (SSSS) and SSSS with quantum dots (QD)

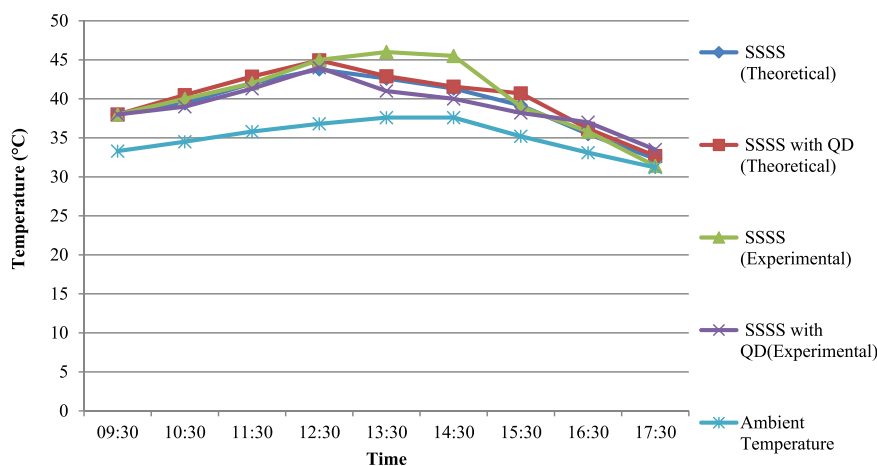


FIGURE 7 Temperature variation inner side of glass (in °C) in single slope solar still (SSSS) and SSSS with quantum dots (QD)

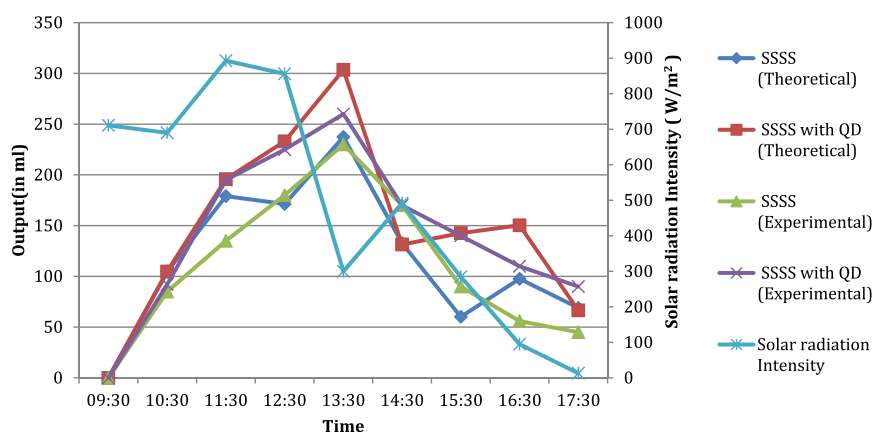


FIGURE 8 Distillate output (in mL) hourly basis in single slope solar still (SSSS) and solar still with quantum dots (QD)

basin, which results enhancement of the temperature of water and hence evaporation of basin water increases (since evaporation is directly depends on temperature, more the temperature more the evaporation from the surface), which in turn increases the distillate output of solar

still which has Pyrex glass QD as basin material in comparison to simple solar still. We have also observed from Figure 7 that there is sudden drop of output for theoretical values at 14:30 hours, this is due to sudden drop in intensity from 856 to 300 W/m<sup>2</sup> because of cloud shading

and calculation was done by assuming  $578 \text{ W/m}^2$  which is average value of  $856$  and  $300 \text{ W/m}^2$  for 14:30 hours.

Figure 9 shows the cumulative output (in ml) experimentally and theoretically in SS and solar still with QD. The total distillate output experimentally in SSSS was 1.031 L and for SSSS with QD was 1.362 L and the total distillate output theoretically in SS was 1.052 L and solar still with QD was 1.211 L. So there is 29.36% increase in distillate output experimentally by using QD in the basin of solar still in comparison to SSSS and 29.94% increase in distillate output by using QD in comparison to simple solar still theoretically. This was happened because when Pyrex glass QD was used, it increases the absorption coefficient of basin which in turn enhances the temperature of water and hence evaporation of basin water increases (since evaporation is directly depend on temperature, more the temperature more the evaporation from the surface) which increases the distillate output of solar still which has Pyrex glass quantum dot as basin material in comparison to simple solar still.

Figure 10 shows the graph of solar still efficiency of SSSS and SSSS with QD. We can see that there is an increase in solar still efficiency of SSSS with QD comparison to simple solar still. With the use of Pyrex glass quantum dots in the basin, the temperature of water has increased, which results in an increase of the temperature difference ( $\Delta T$ ) between glass and water. Due to this, the average increase in solar still efficiency is 74.74% experimentally and 61.03% theoretically in SSSS with Pyrex glass quantum dot in comparison to SSSS.

There was a difference in the experimental and theoretical results of distillate output as shown in Figure 11. This happened because in theoretical modeling, we assume that the set up is completely insulated while practically it is impossible to do perfect insulation of an experimental set-up. The second assumption was that intensity is changing after every 1 hour, but in reality, intensity is changing at every instant due to the change in sun's position. Also, it depends upon climatic condition of the site. We did analysis by considering temperature of water and glass constant for every 1 hour. But in reality, both were

FIGURE 9 Distillate output (in mL) cumulative in SS and solar still with quantum dots (QD)

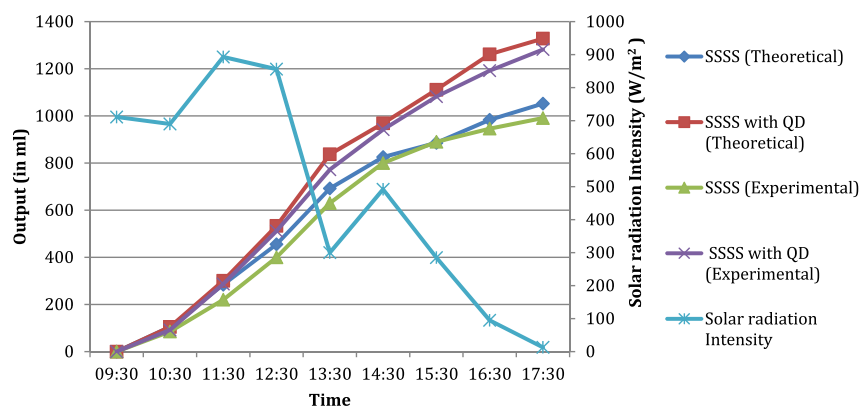
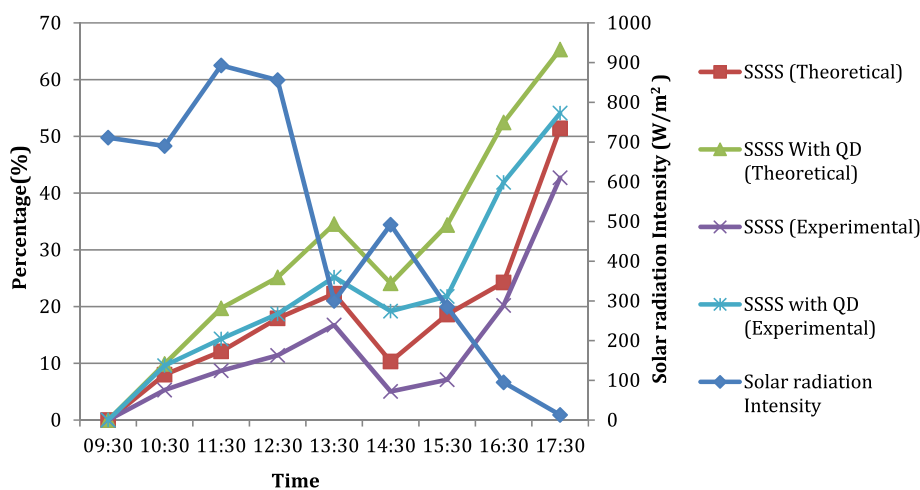


FIGURE 10 Solar still efficiency (hourly basis)



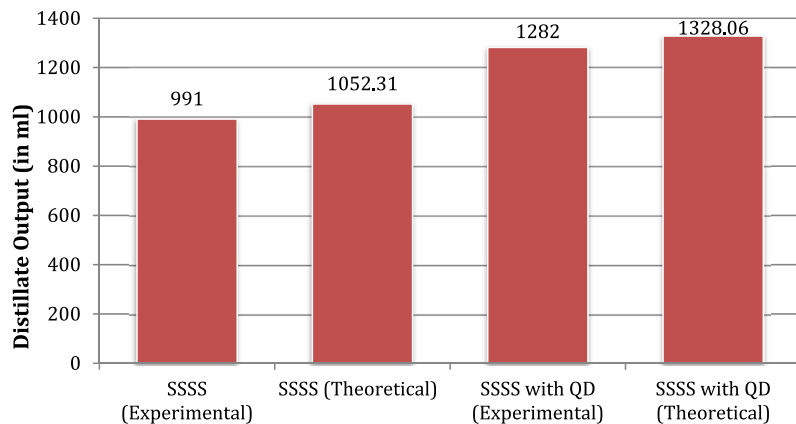


FIGURE 11 Comparison of experimental and theoretical distillate output

changing at every instant due to change in intensity and other climatic parameter like wind velocity, surrounding temperature, etc. Also we assumed wind velocity to be constant for every 1 hour, but practically, it was changing at every instant. Because of these assumptions, the theoretical distillate output slightly differs from experimental distillate output in this study.

## 7 | CONCLUSION

This study investigates the performance analysis of solar still with and without QDs in the tropical climate of India. An experimental setup was developed using two similar solar still, one with Pyrex glass QDs and another without QDs. Both the solar still was tested in real outdoor tropical environment for 1 day. Mathematical model was also developed to validate the experimental results. When Pyrex glass QD with black paint is used, then it gives higher yield comparison to SSSS. Following are the concluding remarks from the study:

1. The distillate output of SSSS is 0.991 L experimentally, whereas the distillate output of SSSS with QD as basin material is 1.282 L experimentally for a depth of 0.02 m.
2. The mathematical analysis results are in better agreement with experimental results, thereby validating the experimental results. The distillate output of SSSS is 1.052 L theoretically, whereas the distillate output of SSSS with QD as basin material is 1.367 L theoretically for a depth of 0.02 m.
3. The percentage increase in distillate output experimentally by using Pyrex glass QDs in the basin of solar still is 29.36% experimentally and 29.94% theoretically in comparison to SSSS.

4. By using Pyrex glass QDs, the solar still efficiency is also increased by 74.74% and 61.03% on experimental and theoretical basis, respectively.
5. Pyrex glass powder QDs with black paint have energy absorbing properties due to which the rate of evaporation of water in the basin is increased which in turn increases the distillate output.
6. The theoretical prediction of distillate outputs from mathematical modeling is a good match with experimental results with a maximum difference in distillate output of approximately 7%.
7. The overall efficiency of SSSS by using Pyrex glass powder QDs has also increased in comparison to simple solar still.
8. The velocity of wind plays an important role in the condensation and evaporation process.

## NOMENCLATURE

$A_s$	area of basin (in $m^2$ )
$P_s$	perimeter of basin (in m)
$L_c$	characteristic length of basin (in m)
$L_b$	thickness of basin (in m)
$L_{in}$	thickness of insulation material (in m)
$M_w$	mass of water (in kg)
$C_w$	specific heat capacity of water (in $J/kg \cdot K$ )
$h_{gw}$	total heat transfer co-efficient between water and glass ( $W/m^2 \cdot K$ )
$h_{radiation, g-w}$	radiation heat transfer coefficient between glass and water ( $W/m^2 \cdot K$ )
$h_{convection, g-w}$	convection heat transfer coefficient between glass and water ( $W/m^2 \cdot K$ )
$h_{evaporation, g-w}$	evaporation heat transfer coefficient between glass and water ( $W/m^2 \cdot K$ )
$h_{ga}$	total heat transfer co-efficient between glass and surrounding ( $W/m^2 \cdot K$ )

$h_{\text{radiation, g-sky}}$	radiation heat transfer coefficient between glass and sky ( $\text{W/m}^2\text{K}$ )
$h_{\text{convection, g-air}}$	convection heat transfer coefficient between glass and outside air ( $\text{W/m}^2\text{K}$ )
$h_{\text{bw}}$	convection heat transfer between basin and water ( $\text{W/m}^2\text{K}$ )
$h_{\text{ba}}$	total heat transfer between basin and outside air ( $\text{W/m}^2\text{K}$ )
$h_{\text{air}}$	average heat transfer co-efficient of air (free convection in $\text{W/m}^2\text{K}$ )
$I(t)_{\text{average}}^i$	average intensity for $i^{\text{th}}$ period ( $\text{W/m}^2$ )
$T_{\text{w}}$	temperature of water (in K)
$T_{\text{g}}$	temperature of glass (in K)
$T_{\text{a}}$	temperature of air (in K)
$T_{\text{b}}$	temperature of basin (in K)
$T_{\text{sky}}$	temperature of sky (in K)
$(MC)_{\text{w}}$	product of mass of water and specific heat of water ( $\text{J/K}$ )
$V$	velocity of air (m/s)
Gr	Grashof number (dimensionless)
Pr	Prantl number (dimensionless)
$k_{\text{b}}$	thermal conductivity of basin ( $\text{W/m}\cdot\text{K}$ )
$k_{\text{w}}$	thermal conductivity of water ( $\text{W/m}\cdot\text{K}$ )
$k_{\text{in}}$	thermal conductivity of wool ( $\text{W/m}\cdot\text{K}$ )
$\nu_{\text{w}}$	kinematic viscosity of water
$\alpha_{\text{w}}$	absorptivity of water or fraction of solar energy absorbed by water (dimensionless)
$\epsilon_{\text{w}}$	emissivity of water (dimensionless)
$\epsilon_{\text{g}}$	emissivity of glass (dimensionless)
$\alpha_{\text{b}}$	absorptivity of basin or fraction of solar energy absorbed by basin (dimensionless)
$\eta_i$	solar still efficiency (for $i^{\text{th}}$ period in %)
$\Delta T$	temperature difference between basin and water (in K)
$\beta_{\text{w}}$	coefficient of volumetric thermal expansion ( $\text{K}^{-1}$ )
$\mu_{\text{w}}$	viscosity of fluid ( $\text{N}\cdot\text{s/m}^2$ )
$\sigma$	Stefan–Boltzmann constant ( $\text{W/m}^2\text{K}^4$ )


## ACKNOWLEDGEMENTS

The authors are grateful to Center for Material for Electronics Technology (C-MET), Pune, Ministry of Electronics and Information Technology, India, for providing all the important resources and materials to successfully conduct this study. Additionally, we are also grateful to Dr. B.B. Kale, Director General, C-MET, Pune, for motivating and encouraging our team to accomplish this study.

## DATA AVAILABILITY STATEMENT

Data sharing not applicable

## ORCID

Pushpendra Kumar Singh Rathore  <https://orcid.org/0000-0003-4363-6298>

## REFERENCES

- World Water Development Report 2020—Water and Climate Change [Internet]. [cited 2021 May 19]. <https://en.unesco.org/themes/water-security/wwap/wwdr/2020>
- Four billion people facing severe water scarcity | Science Advances [Internet]. [cited 2021 May 4]. <https://advances.sciencemag.org/content/2/2/e1500323>
- WHO. *Guidelines for Drinking-Water Quality*. 3rd ed. Switzerland: WHO; 2018 [cited 2020 Nov 26]; [http://www.who.int/water\\_sanitation\\_health/publications/gdwq3/en/](http://www.who.int/water_sanitation_health/publications/gdwq3/en/)
- US EPA O. National Primary Drinking Water Regulations. [cited 2020 Nov 26]; <https://www.epa.gov/ground-water-and-drinking-water/national-primary-drinking-water-regulations>
- Indian Standard for Drinking Water as per BIS specifications (IS 10500-2012) (Second Revision) | India Water Portal [Internet]. [cited 2020 Nov 26]. <https://www.indiawaterportal.org/articles/indian-standard-drinking-water-bis-specifications-10500-1991>
- Darre NC, Toor GS. *Desalination of Water: a Review*. Vol. 4, *Current Pollution Reports*. Germany: Springer; 2018:104-111.
- Fujiwara M, Imura T. Photo induced membrane separation for water purification and desalination using Azobenzene modified anodized alumina membranes. *ACS Nano*. 2015;9(6):5705-5712 [cited 2020 Sep 12]. <https://doi.org/10.1021/nn505970n>
- Boyjoo Y, Pareek VK, Ang M. A review of greywater characteristics and treatment processes [internet]. *Water Sci Technol*. 2013;67:1403-1424.
- Manju S, Sagar N. Renewable energy integrated desalination: a sustainable solution to overcome future fresh-water scarcity in India. *Renew Sustain Energy Rev*. 2017;73:594-609.
- Shatat M, Riffat SB. Water desalination technologies utilizing conventional and renewable energy sources. *Int J Low-Carbon Technol*. 2014;9(1):1-19. [cited 2020 Sep 12] <https://academic.oup.com/ijlct/article/9/1/1/663897>
- Mon M, Bruno R, Ferrando-Soria J, Armentano D, Pardo E. Metal-organic framework technologies for water remediation: towards a sustainable ecosystem. *J Mater Chem A R Soc Chem*. 2018;6:4912-4947. [cited 2020 Sep 12]. <https://pubs.rsc.org/en/content/articlehtml/2018/ta/c8ta00264a>
- Bolisetty S, Peydayesh M, Mezzenga R. Sustainable technologies for water purification from heavy metals: review and analysis. *Chem Soc Rev R Soc Chem*. 2019;48:463-487. [cited 2020 Sep 12]. <https://pubs.rsc.org/en/content/articlehtml/2019/cs/c8cs00493e>
- Lewis NS. Toward cost-effective solar energy use. *Science*. 2007; 315:798-801. [cited 2020 Sep 12]. <https://pubmed.ncbi.nlm.nih.gov/17289986/>
- Chauhan VK, Shukla SK, Tirkey JV, Singh Rathore PK. A comprehensive review of direct solar desalination techniques and its advancements. *J Clean Prod*. 2021;15:284.
- Rathore PKS. An experimental study on solar water heater integrated with phase change material. *Lect Notes Mech Eng*. Singapore: Springer; 2019;347-356. [https://doi.org/10.1007/978-981-13-6416-7\\_33](https://doi.org/10.1007/978-981-13-6416-7_33)
- Arshad K, Janarthanan B, Shanmugan S. Performance of honeycomb double exposure solar still. *Desalin Water Treat*. 2011;

- 26(1–3):260-265. [cited 2020 Sep 12]. <https://www.tandfonline.com/doi/abs/10.5004/dwt.2011.1826>
17. El-Sebaei AA, Aboul-Enein S, El-Bialy E. Single basin solar still with baffle suspended absorber. *Energy Convers Manag.* 2000; 41(7):661-675.
  18. Sohani A, Hoseinzadeh S, Berenjkar K. Experimental analysis of innovative designs for solar still desalination technologies; an in-depth technical and economic assessment. *J Energy Storage.* 2020;33:101862. <https://doi.org/10.1016/j.est.2020.101862>
  19. Suneesh PU, Jayaprakash R, Kumar S, Denkenberger D. Performance analysis of “V”-type solar still with tilt wick and effect of wick coverage. Pham D, editor. *Cogent Eng.* 2017;4(1): 1419791. <https://doi.org/10.1080/23311916.2017.1419791>
  20. Patel M, Patel C, Panchal H. Performance analysis of conventional triple basin solar still with evacuated heat pipes, corrugated sheets and storage materials. *Groundw Sustain Dev.* 2020; 11(April):100387. <https://doi.org/10.1016/j.gsd.2020>
  21. Mahmoud A, Fath H, Ookwara S, Ahmed M. Influence of partial solar energy storage and solar concentration ratio on the productivity of integrated solar still/humidification-dehumidification desalination systems. *Desalination.* 2019;467:29-42.
  22. Chaichan MT, Abaas KI, Kazem HA. Design and assessment of solar concentrator distilling system using phase change materials (PCM) suitable for desertic weathers. *Desalin Water Treat.* 2016;57(32):14897-14907.
  23. Thakur AK, Agarwal D, Khandelwal P, Dev S. Comparative study and yield productivity of nano-paint and nano-fluid used in a passive-type single basin solar still. *Lect Notes Electr Eng.* 2018;435:709-716.
  24. Modi KV, Shukla DL, Ankoliya DB. A comparative performance study of double basin single slope solar still with and without using nanoparticles. *J Sol Energy Eng Trans ASME.* 2019;141(3):031008-1-031008-10.
  25. Modi KV, Jani HK, Gamit ID. Impact of orientation and water depth on productivity of single-basin dual-slope solar still with Al<sub>2</sub>O<sub>3</sub> and CuO nanoparticles. *J Therm Anal Calorim.* 2020; 143:899-913. <https://doi.org/10.1007/s10973-020-09351-1>
  26. Subhedar DG, Chauhan KV, Patel K, Ramani BM. Performance improvement of a conventional single slope single basin passive solar still by integrating with nanofluid-based parabolic trough collector: an experimental study. *Materials Today: Proceedings.* Netherlands: Elsevier Ltd; 2019:1478-1481.
  27. Shanmugan S, Essa FA, Gorjian S, Kabeel AE, Sathyamurthy R, Muthu MA. Experimental study on single slope single basin solar still using TiO<sub>2</sub> nano layer for natural clean water invention. *J Energy Storage.* 2020;30(April):101522. <https://doi.org/10.1016/j.est.2020.101522>
  28. Behura A, Gupta H. Use of nanoparticle-embedded phase change material in solar still for productivity enhancement. *Mater Today Proc.* 2020;45(Part 4):10-13. <https://doi.org/10.1016/j.matpr.2020.06.285>
  29. Malik MZ, Musharavati F, Khanmohammadi S, Khanmohammadi S, Nguyen DD. Solar still desalination system equipped with paraffin as phase change material: exergoeconomic analysis and multi-objective optimization. *Environ Sci Pollut Res.* 2020;28:220-234.
  30. Moshi AAM. Experimental investigation on the performance enhancement of single basin double slope solar still using kanchey marbles as sensible heat storage materials. *Mater Today Proc.* 2021;39:1600-1604. <https://doi.org/10.1016/j.matpr.2020.05.710>
  31. Kabeel AE, Sathyamurthy R, Sharshir SW, et al. Effect of water depth on a novel absorber plate of pyramid solar still coated with TiO<sub>2</sub> nano black paint. *J Clean Prod.* 2019;213:185-191.
  32. Porta-Gándara MA, Fernández-Zayas JL, Chargoy-del-Valle N. Solar still distillation enhancement through water surface perturbation. *Sol Energy.* 2020;196(December 2019):312-318. <https://doi.org/10.1016/j.solener.2019.12.028>
  33. Panchal H. Annual performance analysis of various energy storage materials in the upper basin of a double-basin solar still with vacuum tubes. *Int J Ambient Energy.* 2020;41(4):435-451. <https://doi.org/10.1080/01430750.2018.1472653>
  34. Akash BA, Mohsen MS, Osta O, Elayan Y. Experimental evaluation of a single-basin solar still using different absorbing materials. *Renew Energy.* 1998;14(1–4):307-310.
  35. Zurigat YH, Abu-Arabi MK. Modelling and performance analysis of a regenerative solar desalination unit. *Appl Therm Eng.* 2004 May;24(7):1061-1072.
  36. Chaichan MT, Kazem HA. Author's accepted manuscript. *Case Stud Therm Eng.* 2015;5:151-159. <https://doi.org/10.1016/j.csite.2015.03.009>
  37. Parsa SM, Rahbar A, Koleini MH, Aberoumand S, Afrand M, Amidpour M. A renewable energy-driven thermoelectric-utilized solar still with external condenser loaded by silver/nanofluid for simultaneously water disinfection and desalination. *Desalination.* 2020;480:114354.
  38. Chaichan MT, Kazem HA. Single slope solar distillator productivity improvement using phase change material and Al<sub>2</sub>O<sub>3</sub> nanoparticle. *Sol Energy.* 2018;164:370-381.
  39. Cotta MA. Quantum dots and their applications: what lies ahead? *ACS Appl Nano Mater.* 2020;3(6):4920-4924.
  40. Johnson A, Mu L, Park YH, Valles DJ, Wang H, Xu P, et al. A thermal model for predicting the performance of a solar still with Fresnel lens. 2019;
  41. Duffie JA, Beckman WA, McGowan J. Solar Engineering of Thermal Processes. *Am J Phys.* 1985;53:382-382.
  42. Solar water distillation: the roof type still and a multiple effect diffusion still.—Trove [Internet]. [cited 2021 Jan 13]. <https://trove.nla.gov.au/work/34968478>
  43. Sharma VB, Mullick SC. Estimation of heat-transfer coefficients, the upward heat flow, and evaporation in a solar still. *J Sol Energy Eng.* 1991;113:36-41.
  44. Corcione M. Heat transfer correlations for free convection from upward-facing horizontal rectangular surfaces. *WSEAS Trans Heat Mass Transf.* 2007;2(3):48-60. <http://wseas.us/e-library/transactions/heat/2007/25-637N.pdf>
  45. Grashof Number—an overview|ScienceDirect Topics [Internet]. [cited 2021 Jan 13]. <https://www.sciencedirect.com/topics/earth-and-planetary-sciences/grashof-number>
  46. Emissivity of the Ocean | The Science of Doom [Internet]. [cited 2021 Jan 12]. <https://scienceofdoom.com/2010/12/27/emissivity-of-the-ocean/>
  47. Emissivity Coefficient Materials [Internet]. [cited 2021 Jan 12]. [https://www.engineeringtoolbox.com/emissivity-coefficients-d\\_447.html](https://www.engineeringtoolbox.com/emissivity-coefficients-d_447.html)
  48. Heat Capacity and Water [Internet]. [cited May 19]. [https://www.usgs.gov/special-topic/water-science-school/science/heat-capacity-and-water?qt-science\\_center\\_objects=0#qt-science\\_center\\_objects](https://www.usgs.gov/special-topic/water-science-school/science/heat-capacity-and-water?qt-science_center_objects=0#qt-science_center_objects)
  49. Thermal Expansion—The Physics Hypertextbook [Internet]. [cited 2021 Jan 12]. <https://physics.info/expansion/>

50. Kiselev SP, Vorozhtsov EV, Fomin VM. *Ideal Fluid*; Singapore: Springer; 2017:187-266.
51. Water—Thermal Conductivity [Internet]. [cited 2021 Jan 12]. [https://www.engineeringtoolbox.com/water-liquid-gas-thermal-conductivity-temperature-pressure-d\\_2012.html](https://www.engineeringtoolbox.com/water-liquid-gas-thermal-conductivity-temperature-pressure-d_2012.html)
52. Mineral Wool—an overview | ScienceDirect Topics [Internet]. [cited 2021 Jan 12]. <https://www.sciencedirect.com/topics/engineering/mineral-wool>

**How to cite this article:** Singh PK, Rathore PKS, Shukla SK. Experimental and numerical analysis of solar still using Pyrex glass quantum dot in tropical climate. *Int J Energy Res.* 2022;46(2):937-951. doi: 10.1002/er.7214